Supplementary Materials to "A Decoupled Learning Scheme for Real-world Burst Denoising from Raw Images"

Zhetong Liang[1,2], Shi Guo[1,2], Hong Gu[3], Huaqi Zhang[3], and Lei Zhang[1,2] ⋆

[1] Department of Computing, The Hong Kong Polytechnic University
[2] DAMO Academy, Alibaba Group
[3] vivo Mobile Communication Co., Ltd
{csztliang, csshiguo, cslzhang}@comp.polyu.edu.hk
{guhong, zhanghuaqi}@vivo.com

In this supplementary file, we provide:

1. More visual comparison results of the denoising models on synthetic test set. (Please refer to Section 4.2 in the main paper.)
2. More visual comparison results of the denoising models on real-world testing set, including Real-static and Real-dynamic test sets. (Please refer to Section 4.3 in the main paper.)
3. More results of ablation study, including the comparison among different network architectures and the comparison among different training strategies. (Please refer to Section 4.4 in the main paper.)

1 More Results on Synthetic Test Set

In this section, we give more visual comparison results on the synthetic test set by the compared denoising methods, including VBM4D [4], DNCNN [8], RIDNet [1], KPN [5], TOFlow [7] and the proposed BDNet. Fig. 1 shows the results on Gaussian noise σ=25. Figs. 2, 3 show the results on Gaussian noise σ=50, and Fig. 4 shows the results on Poisson-Gaussian noise with noise levels specified in Eq. (2) in the main paper.

⋆ Corresponding author. This work is supported by the Hong Kong RGC RIF grant (R5001-18).

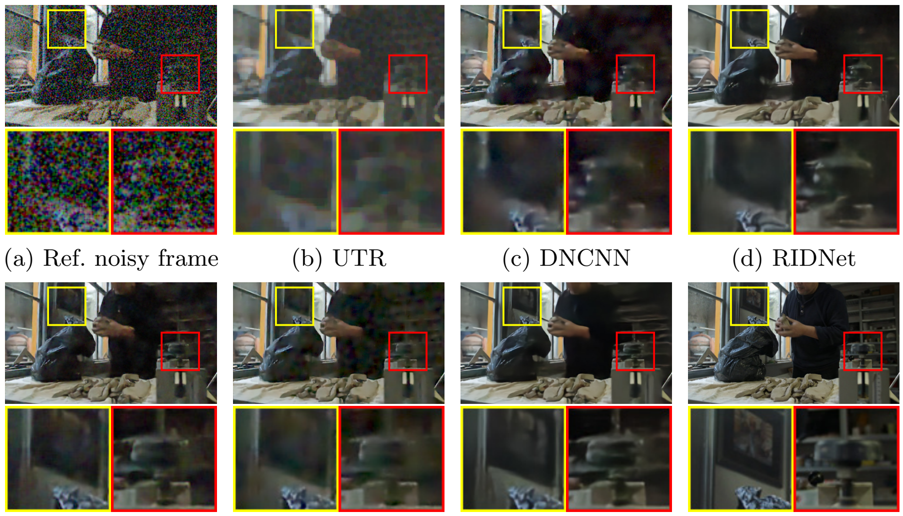

(a) Ref. noisy frame (b) UTR (c) DNCNN (d) RIDNet

(e) KPN (f) TOFlow (g) BDNet (h) ground-truth

Fig. 1: The denoising results of the compared methods on Vimeo-200 test set with Gaussian noise σ=25.

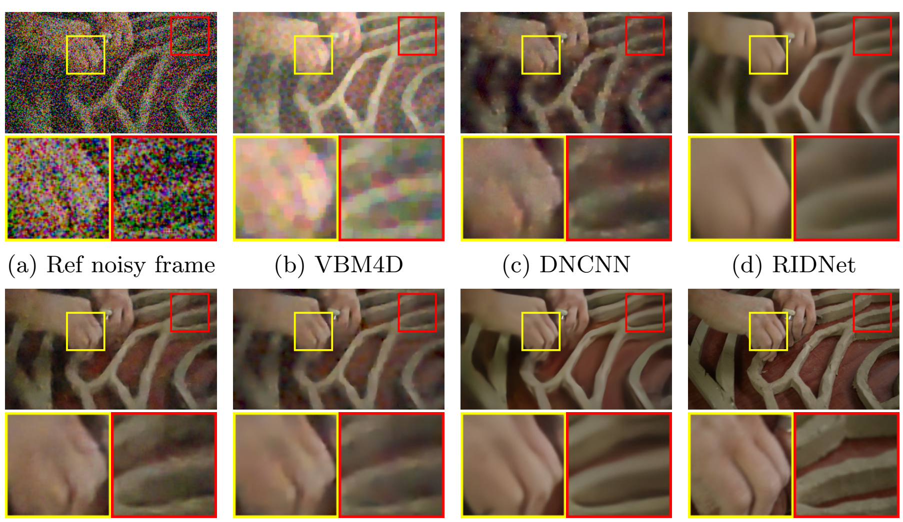

(a) Ref noisy frame (b) VBM4D (c) DNCNN (d) RIDNet

(e) KPN (f) TOFlow (g) BDNet (h) ground-truth

Fig. 2: The denoising results of the compared methods on Vimeo-200 test set with Gaussian noise σ=50.

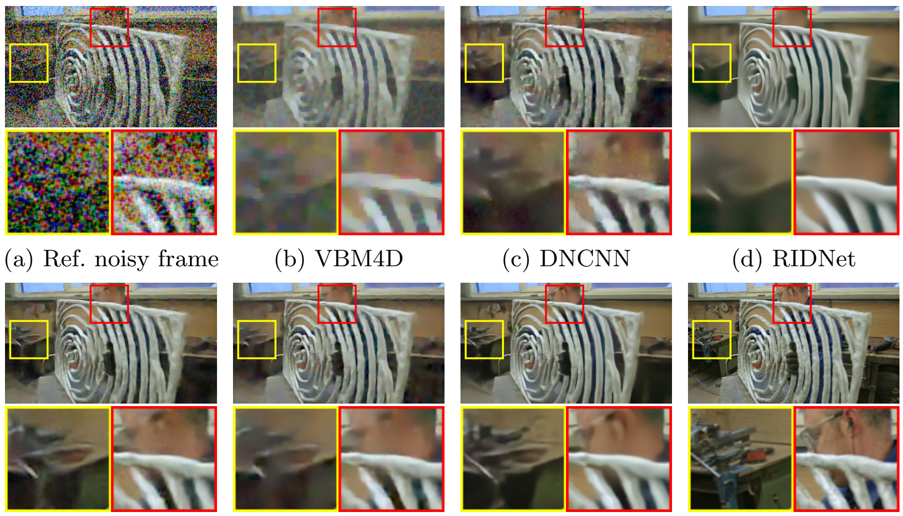

(a) Ref. noisy frame (b) VBM4D (c) DNCNN (d) RIDNet

(e) KPN (f) TOFlow (g) BDNet (h) ground-truth

Fig. 3: The denoising results of the compared methods on Vimeo-200 test set with Gaussian noise σ=50.

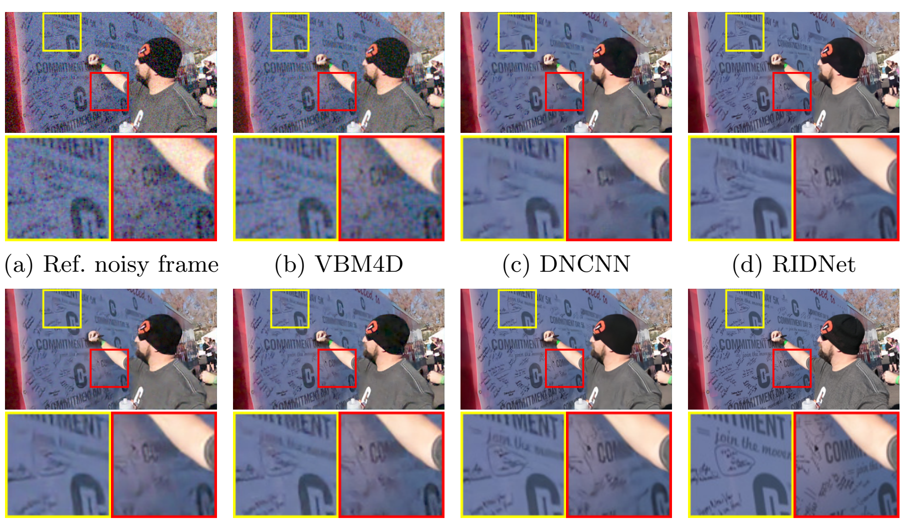

(a) Ref. noisy frame (b) VBM4D (c) DNCNN (d) RIDNet

(e) KPN (f) TOFlow (g) BDNet (h) ground-truth

Fig. 4: The denoising results of the compared methods on Vimeo-200 test set with Poisson-Gaussian noise.

2 More Results on Real-world Testing Sets

In this section, we give more visual comparison results on the real-world testing sets by the compared denoising methods, including UTR [2], M-UNet, M-RIDNet, KPN [5], INN [3] and the proposed BDNet. Fig. 5 shows the results of the compared methods on Real-static test set, while Figs. 6∼8 show the results of the compared methods on Real-dynamic test set.

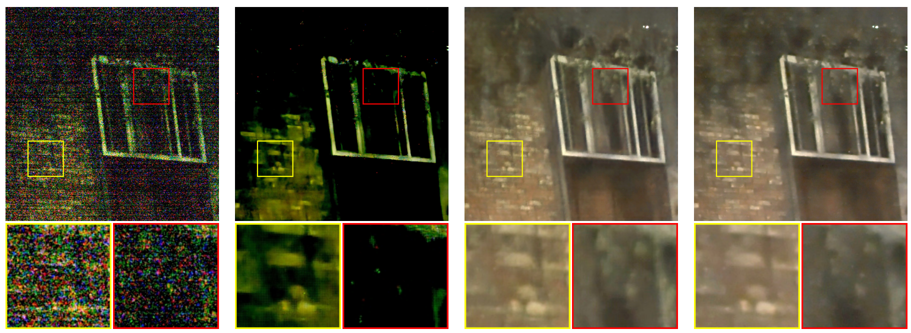
(a) Ref. noisy frame (b) UTR (c) M-UNet (d) M-RIDNet


(e) KPN (f) INN (g) BDNet (h) ground-truth

Fig. 5: The denoising results of the compared methods on Real-static test set.

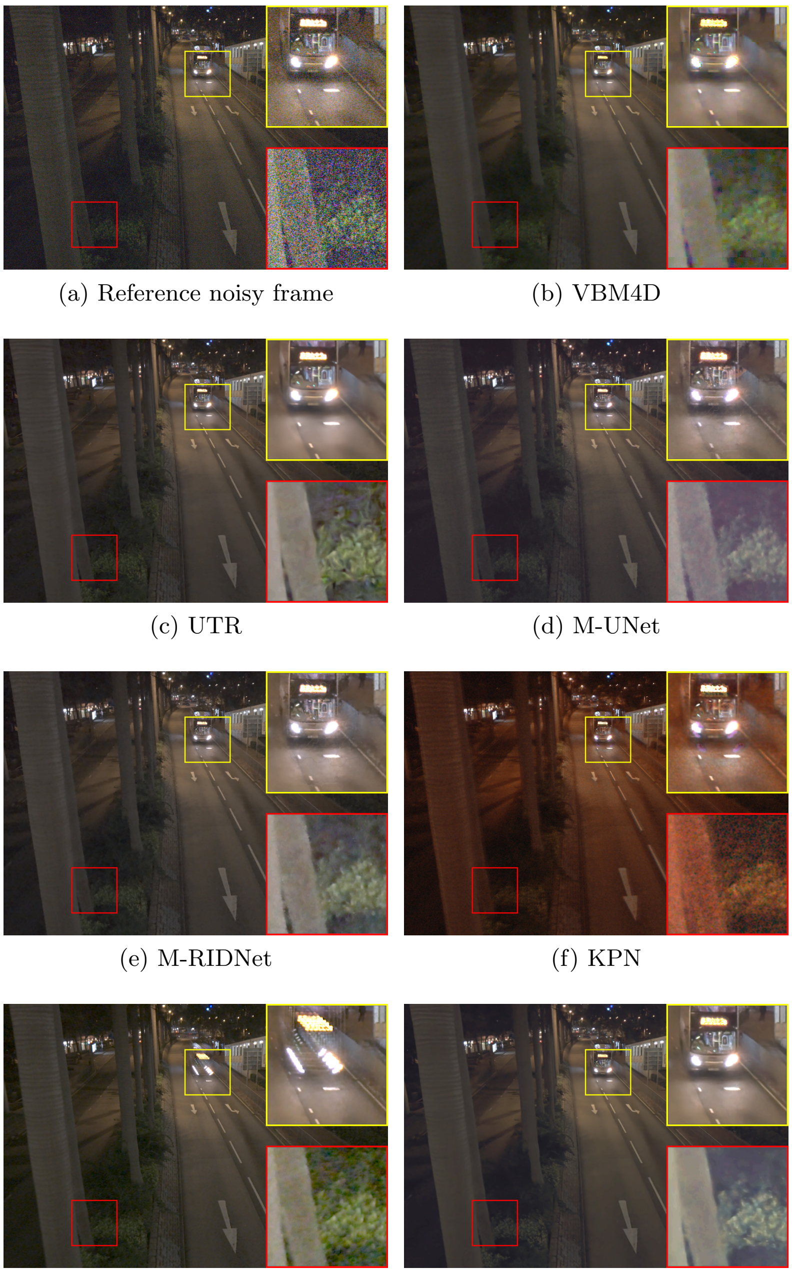

(a) Reference noisy frame (b) VBM4D

(c) UTR (d) M-UNet

(e) M-RIDNet (f) KPN

(g) INN (h) BDNet

Fig. 6: The denoising results of the compared methods on Real-dynamic test set.

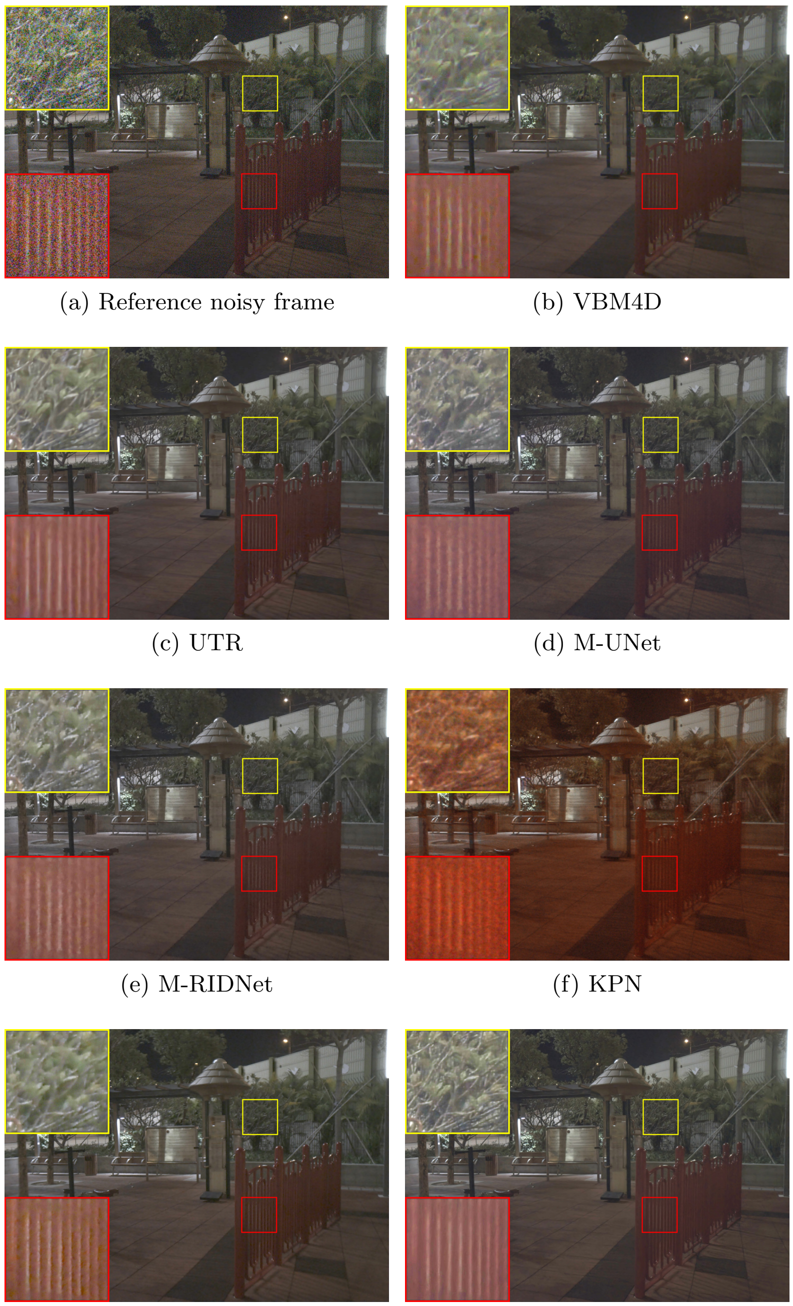

(a) Reference noisy frame (b) VBM4D

(c) UTR (d) M-UNet

(e) M-RIDNet (f) KPN

(g) INN (h) BDNet

Fig. 7: The denoising results of the compared methods on Real-dynamic test set.

(a) Reference noisy frame
(b) VBM4D
(c) UTR
(d) M-UNet
(e) M-RIDNet
(f) KPN
(g) INN
(h) BDNet

Fig. 8: The denoising results of the compared methods on Real-dynamic test set.

3 More Results of Ablation Study

3.1 Different Architectures

We compare the default BDNet with two other network settings. The first network, denoted by BDN-pp, replaces the default PreP and PostP modules by 14 and 12 plain Conv+LReLU blocks (with comparable amount of parameters), respectively, while keeping the TemP module unchanged. This arrangement is to verify the effectiveness of multi-scale and residual structures of PreP and PostP, respectively. The second network, denoted by BDNet-tp, replaces the default TemP module by the SpyNet module [6], while keeping PreP and PostP modules unchanged. This setting examines the effectiveness of alignment operation in feature domain over image domain.

Table 1 shows the quantitative comparison of these network settings on Real-static test set, while Fig. 9 shows a visual comparison on Real-dynamic test set. One can see that the default BDNet obtains much higher PSNR/SSIM scores and reconstructs clearer details than BDNet-pp and BDNet-tp.

Table 1: Quantitative results (PSNR/SSIM) of different network structures on the Real-static test set.

BDNet-pp	BDNet-tp	Default setting
43.18/0.964	42.11/0.963	**45.31/0.971**

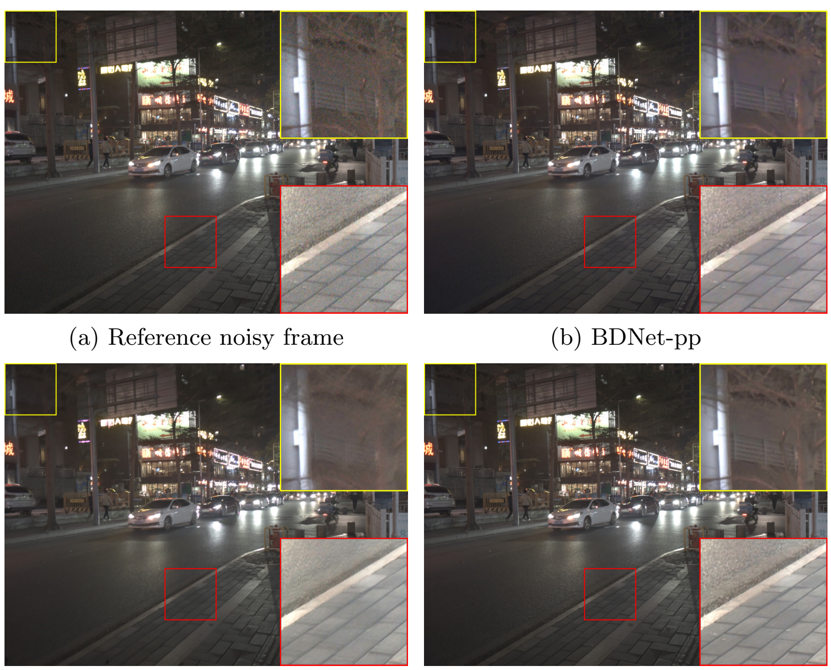

(a) Reference noisy frame (b) BDNet-pp

(c) BDNet-tp (d) BDNet

Fig. 9: The results of the different network structures on Real-dynamic test set.

3.2 Different Learning Schemes

In this subsection, we give more visual comparison results by the compared training strategies, including BDNet-ft, BDNet-at and the default BDNet, on Real-dynamic test set. We can see that BDNet-at causes color shift in the results, as shown in Fig. 10(c) and Fig. 11(c). BDNet-ft produces motion blur in the regions of moving objects, as shown in Fig. 11(b) and Fig. 12(b).

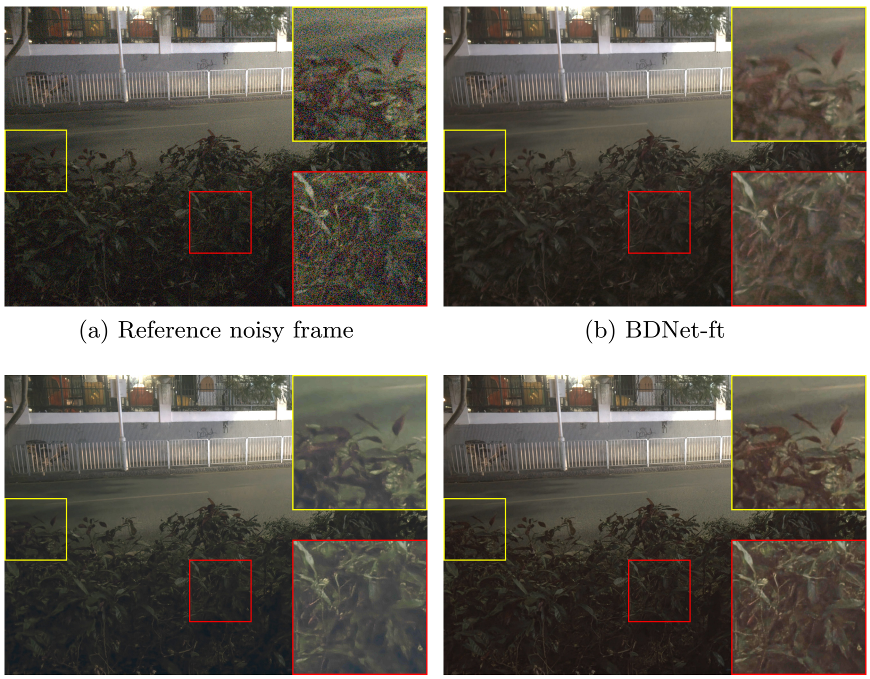

(a) Reference noisy frame (b) BDNet-ft (c) BDNet-at (d) BDNet

Fig. 10: The results of the compared training schemes on Real-dynamic test set.

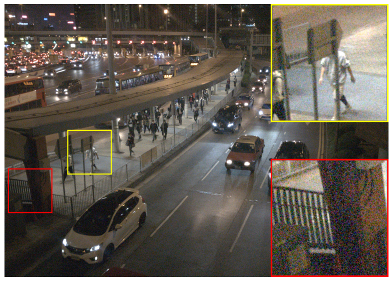

(a) Reference noisy frame

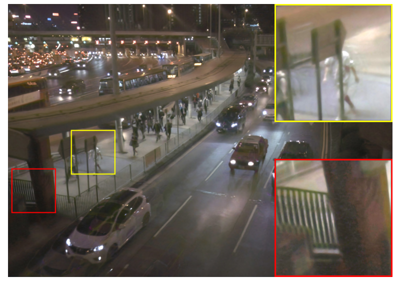

(b) BDNet-ft

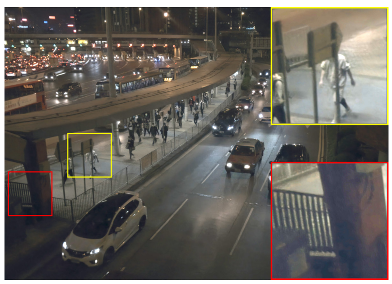

(c) BDNet-at

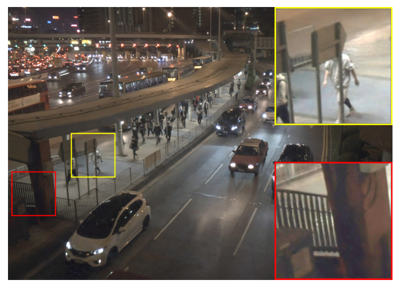

(d) BDNet

Fig. 11: The results of the compared training schemes on Real-dynamic test set.

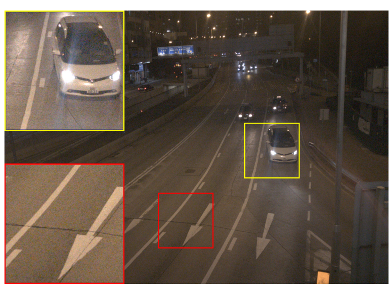

(a) Reference noisy frame

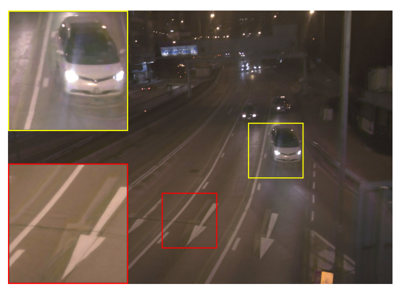

(b) BDNet-ft

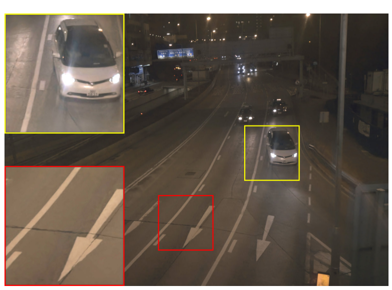

(c) BDNet-at

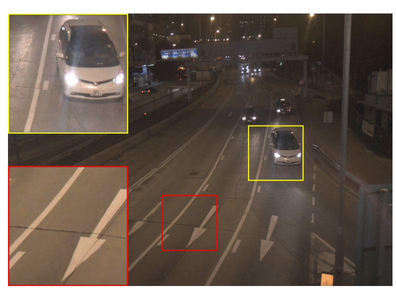

(d) BDNet

Fig. 12: The results of the compared training schemes on Real-dynamic test set.

References

1. Anwar, S., Barnes, N.: Real image denoising with feature attention. In: The IEEE International Conference on Computer Vision (ICCV) (October 2019)
2. Brooks, T., Mildenhall, B., Xue, T., Chen, J., Sharlet, D., Barron, J.T.: Unprocessing images for learned raw denoising. In: IEEE Conference on Computer Vision and Pattern Recognition (CVPR) (2019)
3. Kokkinos, F., Lefkimmiatis, S.: Iterative residual cnns for burst photography applications. In: IEEE Conference on Computer Vision and Pattern Recognition, CVPR 2019, Long Beach, CA, USA, June 16-20, 2019. pp. 5929–5938. Computer Vision Foundation / IEEE (2019)
4. Maggioni, M., Boracchi, G., Foi, A., Egiazarian, K.: Video denoising, deblocking, and enhancement through separable 4-D nonlocal spatiotemporal transforms. IEEE Transactions on Image Processing **21**(9), 3952–3966 (Sep 2012). https://doi.org/10.1109/TIP.2012.2199324
5. Mildenhall, B., Barron, J.T., Chen, J., Sharlet, D., Ng, R., Carroll, R.: Burst denoising with kernel prediction networks. In: Proc. IEEE/CVF Conf. Computer Vision and Pattern Recognition. pp. 2502–2510 (Jun 2018). https://doi.org/10.1109/CVPR.2018.00265
6. Ranjan, A., Black, M.J.: Optical flow estimation using a spatial pyramid network. In: Proceedings of the IEEE Conference on Computer Vision and Pattern Recognition (CVPR) (July 2017)
7. Xue, T., Chen, B., Wu, J., Wei, D., Freeman, W.T.: Video enhancement with task-oriented flow. International Journal of Computer Vision (IJCV) **127**(8), 1106–1125 (2019)
8. Zhang, K., Zuo, W., Chen, Y., Meng, D., Zhang, L.: Beyond a gaussian denoiser: Residual learning of deep CNN for image denoising. IEEE Transactions on Image Processing **26**(7), 3142–3155 (Jul 2017). https://doi.org/10.1109/TIP.2017.2662206